Heliyon 10 (2024) e26804

Contents lists available at ScienceDirect

Heliyon

journal homepage: www.cell.com/heliyon

Research article

Multi-omics landscape analysis reveals the pan-cancer association of arginine biosynthesis genes with tumor immune evasion and therapy resistance

Zhiyong Tan [a,b,c,1], Haihao Li [a,b,c,1], Yinglong Huang [a,b,c,1], Shi Fu [a,b,c,1], Haifeng Wang [a,b,c,*], Jiansong Wang [a,b,c,**]

[a] *Department of Urology, The Second Affiliated Hospital of Kunming Medical University, No. 347, Dianmian Street, Wuhua District, Kunming, 650101, Yunnan, China*

[b] *Urological disease clinical medical center of Yunnan province, The Second Affiliated Hospital of Kunming Medical University, No. 347, Dianmian Street, Wuhua District, Kunming, 650101, Yunnan, China*

[c] *Scientific and Technological Innovation Team of Basic and Clinical Research of Bladder Cancer in Yunnan Universities, The Second Affiliated Hospital of Kunming Medical University, No. 347, Dianmian Street, Wuhua District, Kunming 650101, Yunnan, China*

ARTICLE INFO

Keywords:
Arginine biosynthesis genes
Immune evasion
Pan-cancer

ABSTRACT

Background: The metabolism of arginine, a conditionally essential amino acid, plays a crucial role in cancer progression and prognosis. However, a more detailed understanding of the influence of arginine biosynthesis genes in cancer is currently unavailable.

Methods: We performed an integrative multi-omics analysis using The Cancer Genome Atlas (TCGA) and Gene Expression Omnibus (GEO) databases to determine the characteristics of these genes across multiple cancer types. To measure the overall activity of arginine biosynthesis genes in cancer, we calculated arginine biosynthesis scores based on gene expression.

Results: Our results indicated that the arginine biosynthesis score was negatively correlated with immune-related pathways, immune infiltration, immune checkpoint expression, and patient prognosis, and single-cell data further clarified that patients with high arginine biosynthesis scores showed a reduced proportion of T and B cells in an immune desert tumor microenvironment and were insensitive to immunotherapy. We also identified several potential drugs through the Cancer Therapeutic Response Portal (CTRP) and Genomics of Drug Sensitivity in Cancer (GDSC) databases that could target arginine biosynthesis genes and potentially improve the response rate to immunotherapy in patients with a high arginine biosynthesis fraction.

Conclusion: Overall, our analyses emphasize that arginine biosynthesis genes are associated with immune evasion in several cancers. Targeting these genes may facilitate more effective immunotherapy.

* Corresponding author. Department of Urology, The Second Affiliated Hospital of Kunming Medical University, Yunnan Institute of Urology, Kunming 650101, China.

** Department of Urology, The Second Affiliated Hospital of Kunming Medical University, Yunnan Institute of Urology, Kunming 650101, China.
E-mail addresses: tanzhiyong1@kmmu.edu.cn (Z. Tan), t13085348360@163.com (H. Wang), wangjiansong@kmmu.edu.cn (J. Wang).

[1] as: Co-first authors.

https://doi.org/10.1016/j.heliyon.2024.e26804
Received 21 June 2023; Received in revised form 23 January 2024; Accepted 20 February 2024
Available online 29 February 2024

1. Introduction

Arginine is a conditionally essential amino acid that is mainly available through three pathways: food protein, endogenous synthesis, and organismal protein turnover. It is necessary for protein synthesis, and its metabolism is associated with biological processes such as inflammation, cell growth, and cell activation [1]. Arginine can be catabolized to the end-product NO by nitric oxide synthase, and impaired and/or excessive NO expression can be involved in tumorigenesis and progression by mediating epigenetic modifications, promoting angiogenesis, and activating mitotic pathways and the Wnt/β-catenin pathway [2]. Arginine metabolism and interactions function as mediators of immunosurveillance and affect essential molecules in the tumor microenvironment, such as macrophages and T lymphocytes, thereby inhibiting immunosurveillance [3]. Enhanced arginase activity induces macrophage differentiation from the M1 to M2 type, and M2 macrophages secrete high levels of immunosuppressive cytokines, leading to an increase in immature myeloid cells, suppression of $CD4^+$ and $CD8^+$ T-cell activity, and prevention of dendritic cell maturation, thereby inhibiting immune-mediated antitumor responses. M2 macrophages activated by interleukin (IL)-4 and IL-13 can induce gene coding for arginase type I (ARG1), causing inhibition of T-cell receptor CD3ξ expression and decreased activation of antitumor T cells [4,5]. Simultaneous overexpression of ARG1 allows ARGs to enter the extracellular compartment, where they may sequester extracellular arginine, further increasing immunosuppression [6,7].

Altered arginine metabolism has been reported in various cancers, including malignant melanoma, gastric cancer, breast cancer, and prostate cancer [8–11]. Thus, an in-depth study of arginine biosynthesis genes can provide insights into immune and targeted therapies for patients with tumors. In this study, we comprehensively analyzed the expression of arginine biosynthesis genes in 33 cancers using multi-omics and clinical data and conducted a predictive analysis of the cancers. Pathway enrichment, potential immune checkpoint, immune microenvironment, and immune infiltration analyses were performed to determine the relationship between arginine biosynthesis genes and the response to immunotherapy. Finally, potential therapeutic targets were predicted. In summary, our study provides a better understanding of the biological features and clinical significance of arginine biosynthesis genes in cancers and the implications of targeting these genes as an effective treatment method.

2. Methods

2.1. Datasets and processing

Transcriptome profiles and clinical information data of 33 cancer types, including adrenocortical carcinoma (ACC), bladder urothelial carcinoma (BLCA), breast invasive carcinoma (BRCA), cervical squamous cell carcinoma and endocervical adenocarcinoma (CESC), cholangiocarcinoma (CHOL), colon adenocarcinoma (COAD), rectum adenocarcinoma (READ), lymphoid neoplasm diffuse large B-cell lymphoma (DLBC), esophageal carcinoma (ESCA), glioblastoma multiforme (GBM), head and neck squamous cell carcinoma (HNSC), basal cell carcinoma (BCC), kidney renal clear cell carcinoma (KIRC), kidney renal papillary cell carcinoma (KIRP), acute myeloid leukemia (LAML), brain lower grade glioma (LGG), liver hepatocellular carcinoma (LIHC), lung adenocarcinoma (LUAD), lung squamous cell carcinoma (LUSC), pancreatic adenocarcinoma (PAAD), prostate adenocarcinoma (PRAD), sarcoma (SARC), skin cutaneous melanoma (SKCM), small cell lung cancer (SCLC), stomach adenocarcinoma (STAD), testicular germ cell tumors (TGCT), thyroid carcinoma (THCA), thymoma (THYM), uterine corpus endometrial carcinoma (UCEC), uterine carcinosarcoma (UCS), uveal melanoma (UVM), mesothelioma (MESO), and pheochromocytoma and paraganglioma (PCPG) were accessed from University of California Santa Cruz (UCSC) Xena data portal (https://xenabrowser.net) [12]. Samples with incomplete survival and clinical data were excluded to obtain a total of 11,031 samples, including 719 non-tumor tissues and 10,312 tumor tissues, and transcriptome profiling data of the donated normal tissues were obtained from the Genotype-Tissue Expression (GTEx) project (https://www.gtexportal.org/home/datasets). Differential analysis was performed using the R package limma. Single-nucleotide variant (SNV), copy number variation (CNV), and methylation data were analyzed using the Gene Set Cancer Analysis (GSCA) database (http://bioinfo.life.hust.edu.cn/GSCA/#/).

2.2. Survival analysis and protein-protein interaction network

To assess the relationship between arginine biosynthesis genes and survival outcomes, univariate Cox regression analysis and Kaplan–Meier survival analysis were performed using the R packages survivor and survimer, and visualized using the R package pheatmap. The log-rank test was used to compare survival distributions at a significance level of $p < 0.05$. The protein-protein interaction (PPI) network of arginine biosynthesis genes was established using the STRING database (https://cn.string-db.org/) [13] to reveal the interactions between genes, with parameters set as the minimum required interaction score >0.4.

2.3. Arginine biosynthesis score and functional enrichment analysis

The ssGSEA method in the R package GSVA was used to calculate the arginine biosynthesis scores for the transcriptomic data of each cancer type separately, referring to the study by Hänzelmann et al. [14]. Gene set enrichment analysis (GSEA) was performed using the R package clusterProfiler to explore the differences in functions and pathways associated with the arginine biosynthesis score. On the basis of a set of 50 human cancer marker pathway genes from the Molecular Signature Database (MSigDB) (http://www.gsea-msigdb.org/gsea/index.jsp), the gene set variation analysis (GSVA) scores of all tumors were calculated using the ssGSEA method in the R package GSVA, after which the correlations with arginine biosynthesis scores were visualized by creating a heatmap with the R

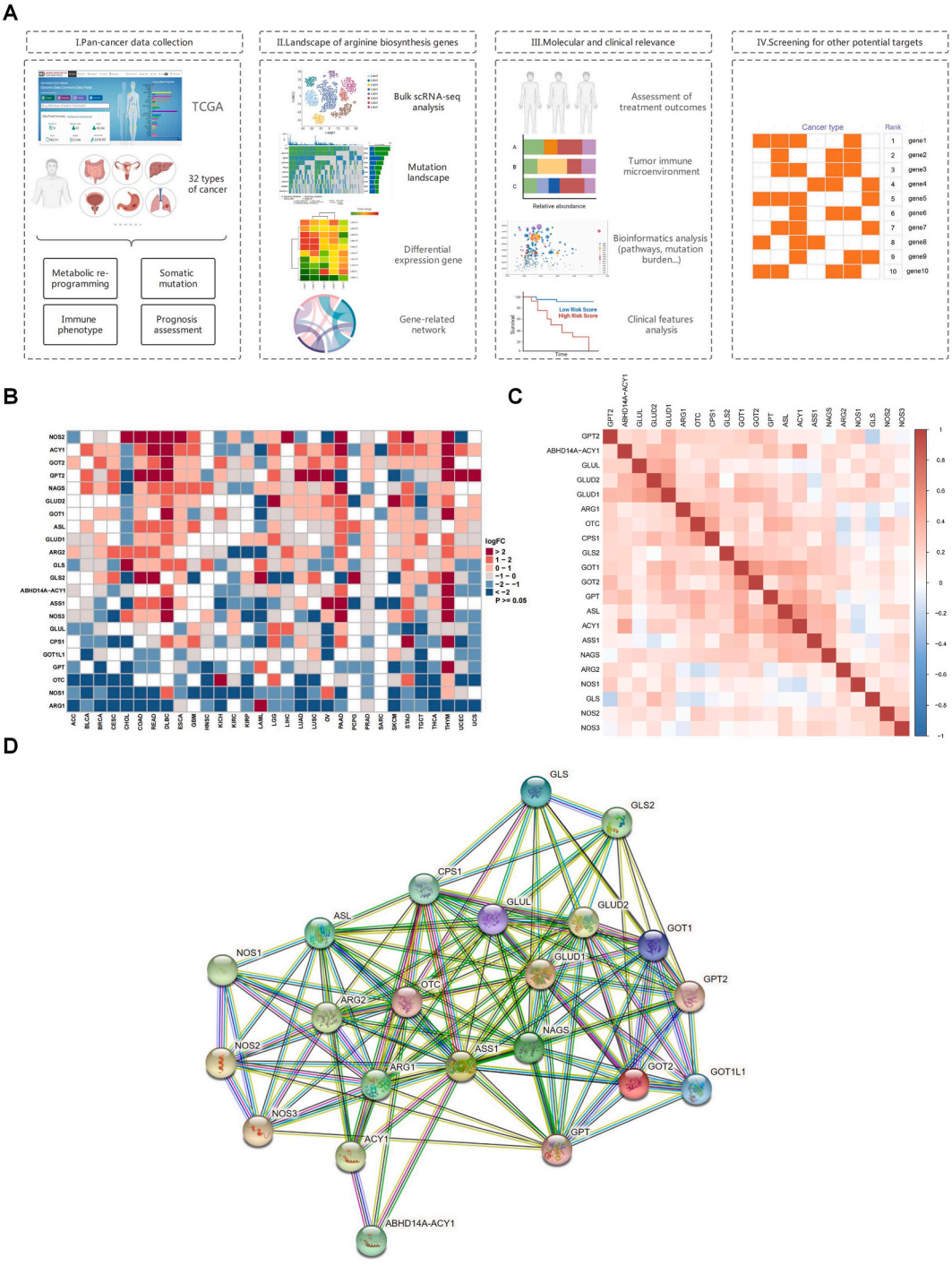

Fig. 1. Arginine biosynthesis genes expression comparison across cancer types and genes. (A) Flow chart of the study. (B) Heatmap for comparing the expressions between all arginine biosynthesis genes between tumor and normal tissue by R package corplot. White represents $p \geq 0.05$; red indicates logFC>0; blue indicates logFC<0; the darker the color, the larger the value of |logFC|. (C) Heatmap for correlation matrix of arginine biosynthesis genes expression across cancer types. Red indicates a positive correlation; blue indicates a negative correlation; the darker the color, the stronger the correlation. (D) Protein-protein interaction network of arginine biosynthesis genes. (For interpretation of the references to color in this figure legend, the reader is referred to the Web version of this article.)

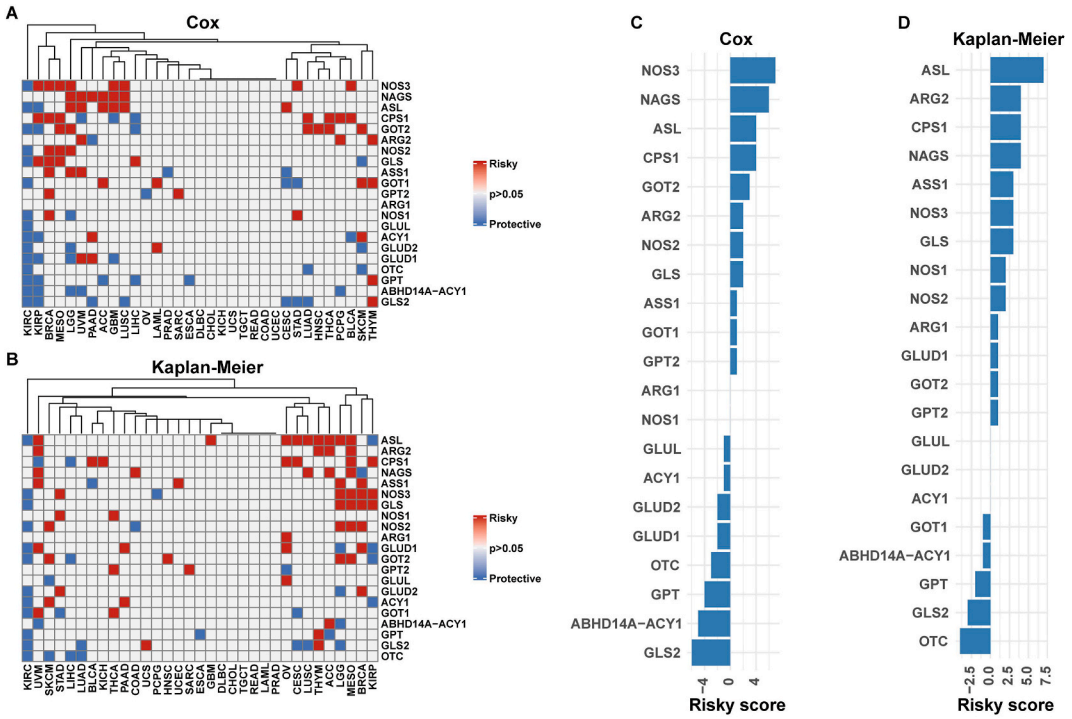

Fig. 2. Expression of arginine biosynthesis genes was associated with prognosis in pan-caners. (A) Heatmaps for univariate cox regression analysis of arginine biosynthesis genes across cancer types. Red represents risky factors; blue represents protective factors; white indicates $p > 0.05$. (B) Kaplan-Meier analysis of arginine biosynthesis genes across cancer types. Red represents risky factors; blue represents protective factors; white indicates $p > 0.05$. (C) Bar plots for risky score calculated based on univariate cox regression analysis. (D) Kaplan-Meier analysis of arginine biosynthesis genes in pan-cancer. (For interpretation of the references to color in this figure legend, the reader is referred to the Web version of this article.)

package Pheatmap.

2.4. Tumor microenvironment and immune infiltration analysis

To demonstrate the correlation between arginine biosynthesis scores and the tumor immune microenvironment in terms of immunity, matrix/metastasis, DNA damage repair, and other related pathways, we referred to the study by Zeng et al. [15], and presented a heat map using the R package ggplot2. Immune cell infiltration data were collected from the ImmuCellAI database (http://bioinfo.life.hust.edu.cn/ImmuCellAI#!/) and the Tumor Immune Estimation Resource 2 (TIMER2) database (http://timer.comp-genomics.org/) for each cancer type, and their associations with the arginine biosynthesis score were assessed. We also extracted data for the expression levels of five immune check loci (PDCD1, LAG3, CD274, CTLA-4, and TIGIT) across cancer types and assessed their associations with arginine biosynthesis scores. Differences in gene mutations between the high- and low-score groups in SKCM were analyzed using the maftools R package, and we selected the top ten genes according to mutation frequency in the two groups, which may be partly responsible for the different responses of patients to immunotherapy.

2.5. Single-cell RNA-seq analysis

Four single-cell datasets containing information on immunotherapeutic responses, namely, GSE115978, GSE120575, GSE123813, and GSE145281, were downloaded from the Tumor Immune Single-cell Hub (TISCH) portal (http://tisch.comp-genomics.org/) [16] to reveal the cell types and arginine biosynthesis score distribution characteristics in SKCM, BCC, and BLCA, and their associations with the immune microenvironment and immunotherapeutic response. The data were filtered and analyzed using the R package Seurat and cells with the following parameters were included: more than 200 genes, less than 7500 genes, and less than 5% of mitochondrial genes. In subsequent processing, we normalized the scRNA-seq data using ScaleData, reduced the dimensionality using the RunUMAP function, identified differentially expressed genes in different clusters using FindAllMarkers, and performed cluster annotation using the R package singleR combined with manual adjustment.

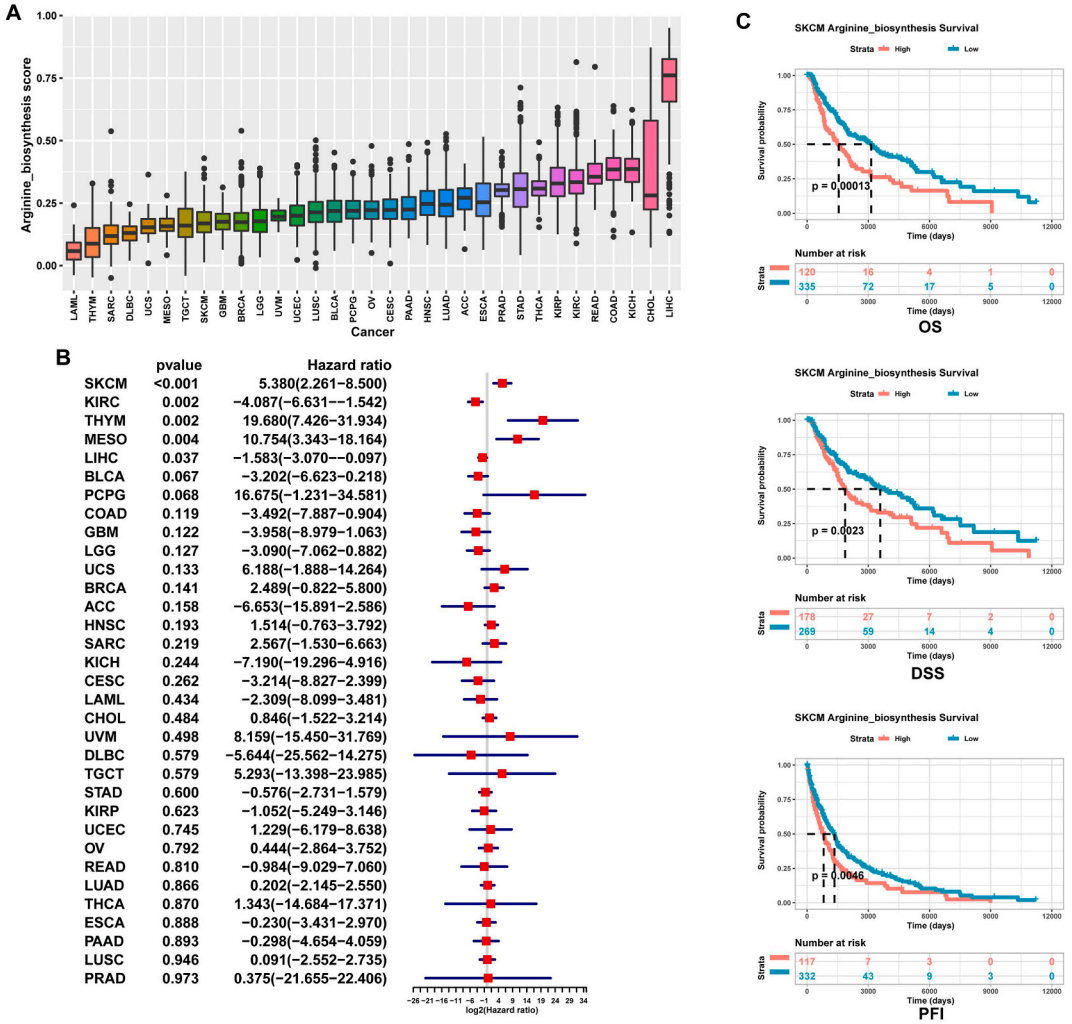

Fig. 3. Arginine biosynthesis score can be used as a prognostic factor of cancers. (A) Bar plot for distribution of arginine biosynthesis score in pan-cancer. (B) Forest plot for univariate regression analysis of arginine biosynthesis score in pan-cancer. (C) Kaplan-Meier plots showing overall survival (OS), disease-specific survival (DSS), and progression-free interval (PFI) rates for high and low arginine biosynthesis scores in SKCM.

2.6. Prediction of immunotherapy response and targeted drugs

To validate the valence of arginine biosynthesis scores in predicting survival outcomes and immunotherapeutic responses, samples containing transcriptome data and the data for therapeutic responses to immunotherapies, including PD-1 and PD-L1 blockade, were obtained as external datasets from the study by Motzer et al. [17] and the GEO database (https://www.ncbi.nlm.nih.gov/geo/). To further identify the potential effect of arginine biosynthesis scores on the effects of chemotherapy, the IC50 values of drugs were extracted using the Genomics of Drug Sensitivity in Cancer (GDSC) (https://www.cancerrxgene.org/) and Cancer Therapeutics Response Portal (CTRP) (https://portals.broadinstitute.org/ctrp.v2.1/) with the R package oncoPredict. Correlations between drug IC50 values and arginine biosynthesis scores were evaluated using Pearson's correlation analysis to detect targeted drugs.

2.7. Quantitative real-time polymerase chain reaction assays

We collected 10 cancerous and 10 peri-carcinomatous tissue samples from patients with BLCA at The Second Affiliated Hospital of Kunming Medical University. Informed consent was obtained from all participants. Total RNA was extracted from the 20 samples using the TRIzol reagent (Life Technology, CA, USA) according to the manufacturer's instructions. The RNAs were then reverse-transcribed into complementary DNA (cDNA) using a FastQuant RT Kit (TIANGEN) [18]. Glyceraldehyde 3-phosphate dehydrogenase (GAPDH) was used as the internal control. The $2^{-\Delta\Delta Ct}$ method was used to determine relative gene expression levels. Supplementary Table 1 lists all the primers used.

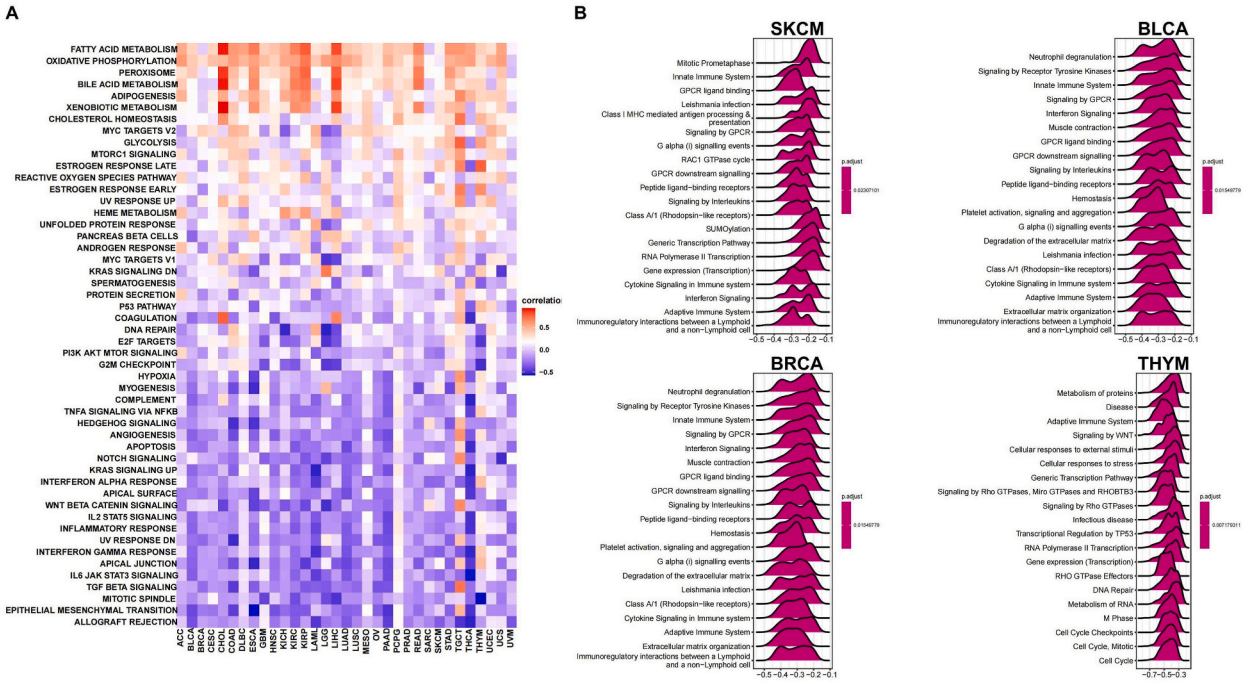

Fig. 4. Arginine biosynthesis score is negatively correlated with immune-related pathways. (A) Heatmap for correlation analysis between arginine biosynthesis score and GSVA enrichment pathway score in pan-cancer. Red indicates a positive correlation; blue indicates a negative correlation; the darker the color, the stronger the correlation. (B) Ridge plot for GSEA analysis of the Reactome pathway for arginine biosynthesis score in SKCM, BLCA, BRCA, and THYM. The purple color indicates p.adjust<0.05; the number at the bottom represents the correlation coefficient, and less than 0 indicates a negative correlation. (For interpretation of the references to color in this figure legend, the reader is referred to the Web version of this article.)

2.8. Immunohistochemistry staining

The tissue slices were baked at 65 °C for 2 h, followed by dewaxing and antigen retrieval. Endogenous enzymes were blocked by treatment with a 3% hydrogen peroxide solution for 10 min at room temperature. The slices were rinsed three times in phosphate buffer solution (PBS) for 3 min each and then blocked with bovine serum albumin. The primary antibody was applied and incubated overnight at 4 °C. After washing the slices three times with PBS for 5 min each, the secondary antibody was added and the slices were incubated at 37 °C for 30 min. Diaminobenzidine was used for color rendering for 5–10 min, followed by hematoxylin staining for 3 min [19]. The slices were observed under a microscope, and the integrated optical density (IOD) was measured using Image Pro Plus 6.0 image software. Relative expression was presented as the average optical density (IOD/positive staining area).

2.9. Statistical analysis

All statistical analyses were performed using R v4.1.1 (https://cran.r-project.org/). Correlations between two variables were assessed using Pearson's or Spearman's correlation analysis, and differences in arginine biosynthesis scores between the responding and non-responding groups were compared using a two-sided Wilcoxon test. The false discovery rate (FDR) was calculated using the Benjamini-Hochberg process (B–H). This work was reported in accordance with the REMARK criteria. * indicates $p \leq 0.05$, ** indicates $p \leq 0.01$, *** indicates $p \leq 0.001$, and **** indicates $p \leq 0.0001$. Statistical significance was set at $P < 0.05$. difference.

3. Results

3.1. The pan-cancer landscape of arginine biosynthesis gene expression and mutation

In the present study, we established a four-step computational framework to elucidate the pan-cancer characteristics of arginine biosynthesis genes, their roles in immunotherapy, and their potential therapeutic targets (Fig. 1A). First, we collected 22 arginine biosynthesis genes from the Kyoto Encyclopedia of Genes and Genomes (KEGG) database (https://www.kegg.jp/entry/map00220), including argininosuccinate lyase (ASL), ornithine carbamoyltransferase (OTC), argininosuccinate synthase 1 (ASS1), arginase-2 (ARG2), arginase-1 (ARG1), nitric oxide synthase 1 (NOS1), nitric oxide synthase 2 (NOS2), nitric oxide synthase 3 (NOS3), glutaminase kidney isoform 2 (GLS2), glutaminase kidney isoform (GLS), glutamate-ammonia ligase (GLUL), glutamate dehydrogenase 2

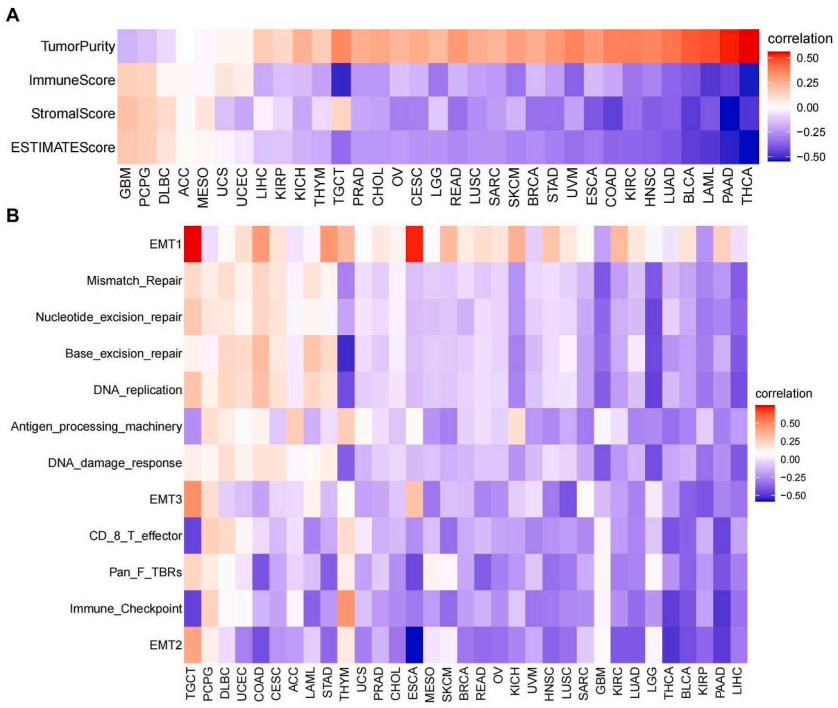

Fig. 5. Arginine biosynthesis score is negatively associated with TME. (A) Heatmap for correlation analysis between arginine biosynthesis score and ESTIMATE Score and TumorPurity in pan-cancer. Red indicates a positive correlation; blue indicates a negative correlation; the darker the color, the stronger the correlation. (B) Heatmap for correlation analysis between arginine biosynthesis score and TME-related pathways in pan-cancer. Red indicates a positive correlation; blue indicates a negative correlation; the darker the color, the stronger the correlation. (For interpretation of the references to color in this figure legend, the reader is referred to the Web version of this article.)

(GLUD2), glutamate dehydrogenase 1 (GLUD1), carbamoyl-phosphate synthase 1 (CPS1), aspartate aminotransferase 1 (GOT1), glutamic-oxaloacetic transaminase 1 like 1 (GOT1L1), aspartate aminotransferase 2 (GOT2), alanine aminotransferase 2 (GPT2), glutamic–pyruvic transaminase (GPT), N-acetyl glutamate synthase (NAGS), aminoacylase-1 (ACY1), and ABHD14A-ACY1. The complexity heatmap revealed that the expression levels of arginine biosynthesis genes differed between normal and tumor tissues in most cancer types (Fig. 1B). The expression of ARG1 was downregulated in several cancers, especially DLBC, but was upregulated in LAML ($p < 0.05$). Further correlation analysis of arginine biosynthesis genes showed that the expression of most genes was positively correlated (Fig. 1C). We constructed a PPI network of arginine biosynthesis genes, as shown in Fig. 1D. Mutations and methylation patterns of arginine biosynthesis genes in various cancers are shown in Supplementary Figs. 1–3. The results of the SNV analysis indicated that missense mutations and single-nucleotide polymorphisms were the most frequent variant types, and NOS1 was the most frequently mutated gene in SKCM (up to 97%). In addition, CNVs in arginine biosynthesis genes occurred in all cancer types, with heterozygous gene amplification and heterozygous deletions being the most frequently observed types of CNVs. Finally, Spearman correlation analysis showed that DNA methylation was negatively correlated with the mRNA expression of arginine biosynthesis genes ($P < 0.05$).

3.2. *Expression of arginine biosynthesis genes was associated with the prognosis of different types of cancers prognosis*

To explore the critical role of arginine biosynthesis genes in tumor prognosis, we conducted univariate Cox regression and Kaplan–Meier survival analyses. The results are shown in Fig. 2. The results of the two analyses were not entirely consistent, and arginine biosynthesis genes were associated with the prognosis of most cancers and played various roles in the prognosis of different cancer types. However, no correlations were observed in TGCT, DLBC, CHOL, and READ. The expression levels of most arginine biosynthesis genes were positively correlated with the prognosis in patients with KIRC, whereas GLS2, GPT, and ARG2 were recognized as risk factors for prognosis among patients with THYM (Fig. 2A and B; $p < 0.05$). Each gene's hazard ratio value was extracted separately; risk factors were ascribed +1 and protective factors were ascribed −1. The risk scores were calculated by summation, which revealed that NOS3, NAGS, ASL, CPS1, GOT2, ARG2, NOS2, GLS, ASS1, and GPT2 can be considered risk factors for tumor prognosis, while OTC, GPT, ABHD14A- ACY1, GLS2 were protective factors; thus, NOS3 and ASL were the most significant risk factors based on risk scores (Fig. 2C and D).

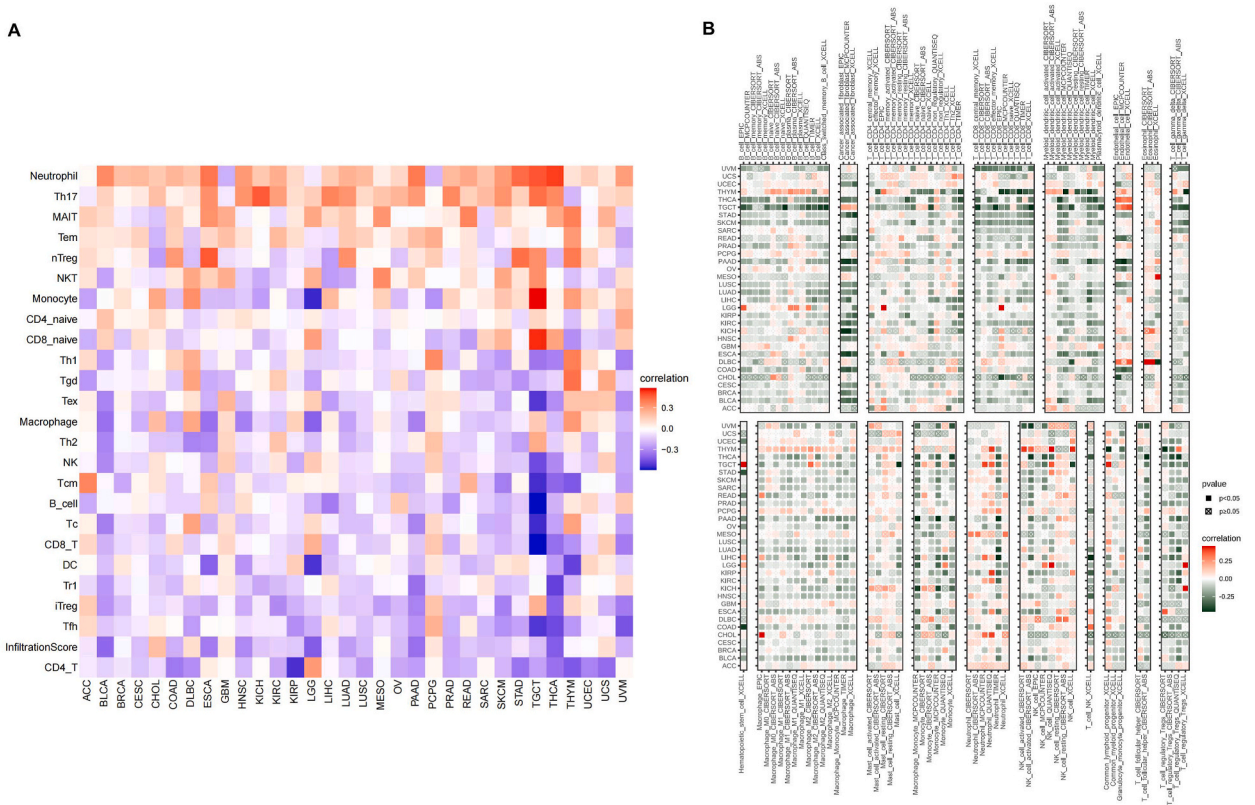

Fig. 6. Higher arginine biosynthesis score confers lower immune infiltration in pan-cancer. Heatmaps for correlation analysis between arginine biosynthesis score and immune infiltration across cancer types based on ImmuCellAI database (A) and TIMER2 database (B). Red indicates a positive correlation; blue and green indicate a negative correlation; the darker the color, the stronger the correlation. (For interpretation of the references to color in this figure legend, the reader is referred to the Web version of this article.)

3.3. Arginine biosynthesis score is a risk factor for survival in specific cancer types

After identifying arginine biosynthesis genes as prognostic risk factors for multiple cancers, we calculated arginine biosynthesis scores to comprehensively estimate the pan-cancer effect of arginine biosynthesis genes. We calculated the arginine biosynthesis scores for each of the 33 cancer types, as shown in Fig. 3A: the LAML samples showed the lowest mean arginine biosynthesis scores, whereas the LIHC samples showed significantly higher mean arginine biosynthesis scores than the other cancer types. Univariate Cox regression analysis showed that the arginine biosynthesis score was a prognostic factor in patients with SKCM, KIRC, THYM, and MESO, particularly as a protective factor against KIRC (Fig. 3B) ($P < 0.01$). Here, we selected SKCM as the target dataset and proceeded to perform Kaplan–Meier analysis, dividing samples into two groups according to the best cutoff value calculated by the surv_cutpoint function in the R survminer package. We found that patients with low arginine biosynthesis scores had better overall survival (OS), disease-specific survival (DSS), and progression-free interval (PFI) ($P < 0.005$), indicating that the score could serve as a prognostic predictor (Fig. 3C).

3.4. Arginine biosynthesis score is negatively correlated with immune-related pathways that affect the tumor microenvironment

For functional annotation of arginine biosynthesis genes, we performed a correlation analysis of arginine biosynthesis scores with GSVA enrichment pathway scores in all cancer types. We found that arginine biosynthesis scores were negatively correlated with multiple tumorigenic and immune-related pathways, such as the PI3K-Akt-mTOR signaling pathway, Notch signaling pathway, Wnt β-catenin signaling pathway, IL6 Jak/Stat3 signaling pathway, and TGF-β signaling pathway (Fig. 4A). GSEA to identify the most significant enrichment pathways for arginine biosynthesis scores was also conducted for individual cancers, with the SKCM, BLCA, BRCA, and THYM cohorts chosen for analysis, and the results were consistent with those obtained in GSVA. Both cell cycle and immune-related pathways were negatively correlated with arginine biosynthesis scores ($p < 0.05$) (Fig. 4B), which implies that high arginine biosynthesis scores may indicate an immunosuppressed tumor microenvironment. Differences in the tumor immune microenvironment between the high- and low-score groups were investigated by measuring the Stromal Score, Immune Score, ESTIMATE Score [20], and TumorPurity, and the outcomes are presented in Fig. 5A. Samples with higher arginine biosynthesis scores had higher tumor purity and showed significant suppression of the tumor immune microenvironment. In contrast, the opposite trend

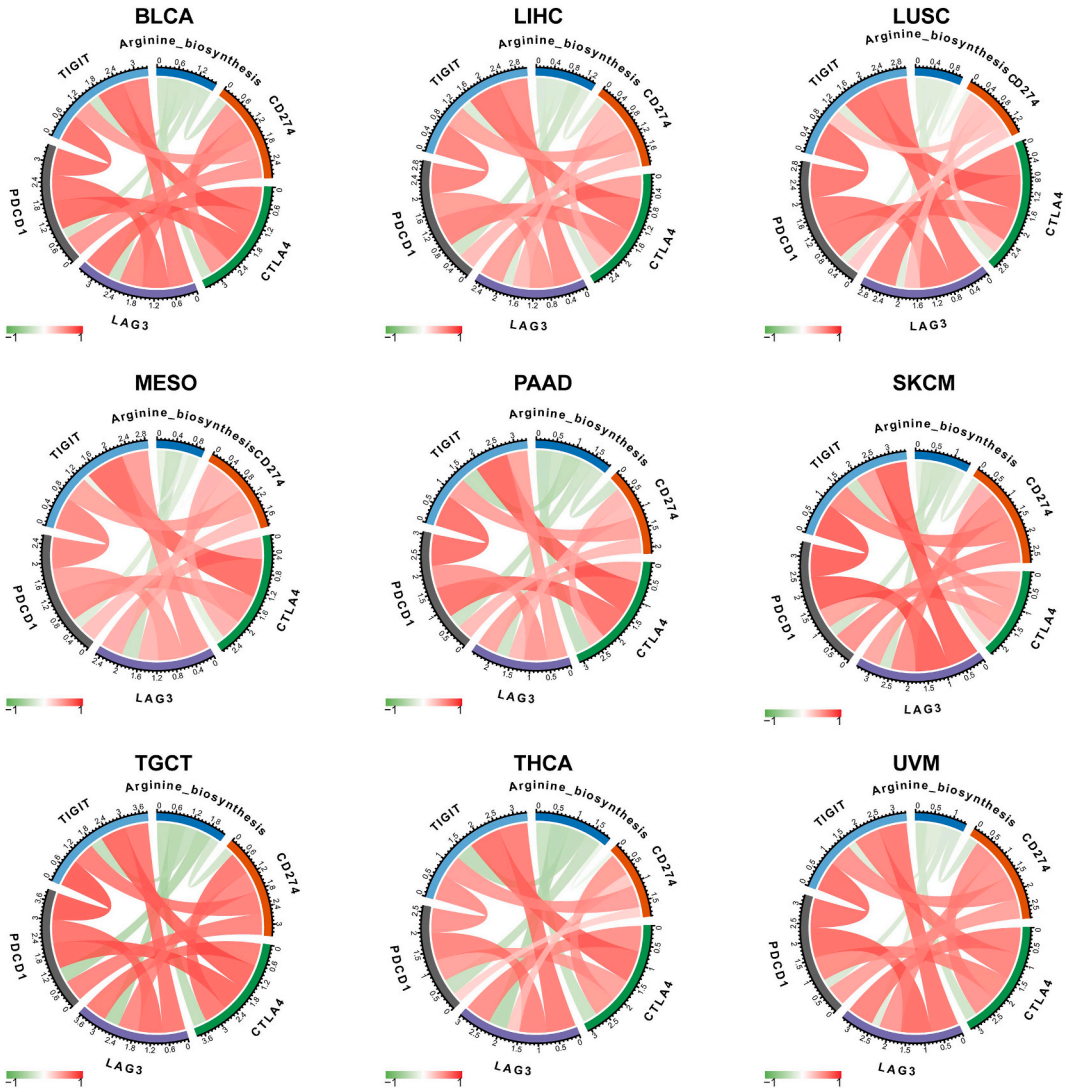

Fig. 7. The chord diagram shows that the arginine biosynthesis score negatively correlates with immune checkpoints in multiple cancers. Red indicates a positive correlation; green indicates a negative correlation; the darker the color, the stronger the correlation. (For interpretation of the references to color in this figure legend, the reader is referred to the Web version of this article.)

was observed for GBM and PCPG. We also assessed the correlation between the arginine biosynthesis score and tumor immune microenvironment by referring to the method described by Zeng et al. [15], and the arginine biosynthesis score was negatively related to immune-related pathways (Antigen_processing_machinery, Immune_Checkpoint, CD_8_T_effector) and stromal/metastasis-related pathways (EMT1, EMT2, EMT3, Pan_F_TBRs) in a variety of cancers (Fig. 5B).

3.5. Arginine biosynthesis score is related to immune infiltration, potential immune checkpoint blockade response, and genetic mutations

Subsequently, we performed immune infiltration analysis using immune cell infiltration data from the two database sources separately, and the results clearly indicated that the percentage of neutrophils was higher in samples with higher arginine biosynthesis fractions. However, the percentages of infiltration of natural killer (NK) cells, B cells, T cells, macrophages, and dendritic cells were lower in samples with higher arginine biosynthesis fractions, and the percentage of tumor-associated fibroblasts (CAFs) and arginine biosynthesis scores were inversely correlated (Fig. 6A and B). Thus, we hypothesized that patients with high arginine biosynthesis scores had an immune desert-type tumor microenvironment, which may be associated with tumor immune evasion and immunotherapy resistance. Therefore, to investigate the effect of the arginine biosynthesis score on the tumor immunotherapy response, we examined the correlation between the arginine biosynthesis score and immune check loci, as shown in Fig. 7. In various tumor types, arginine biosynthesis scores showed significant negative associations with the expression levels of immune check loci, such as TIGIT, PDCD1, LAG3, CTLA4, and CD274. Therefore, we speculate that patients with high arginine biosynthesis scores are more likely to be

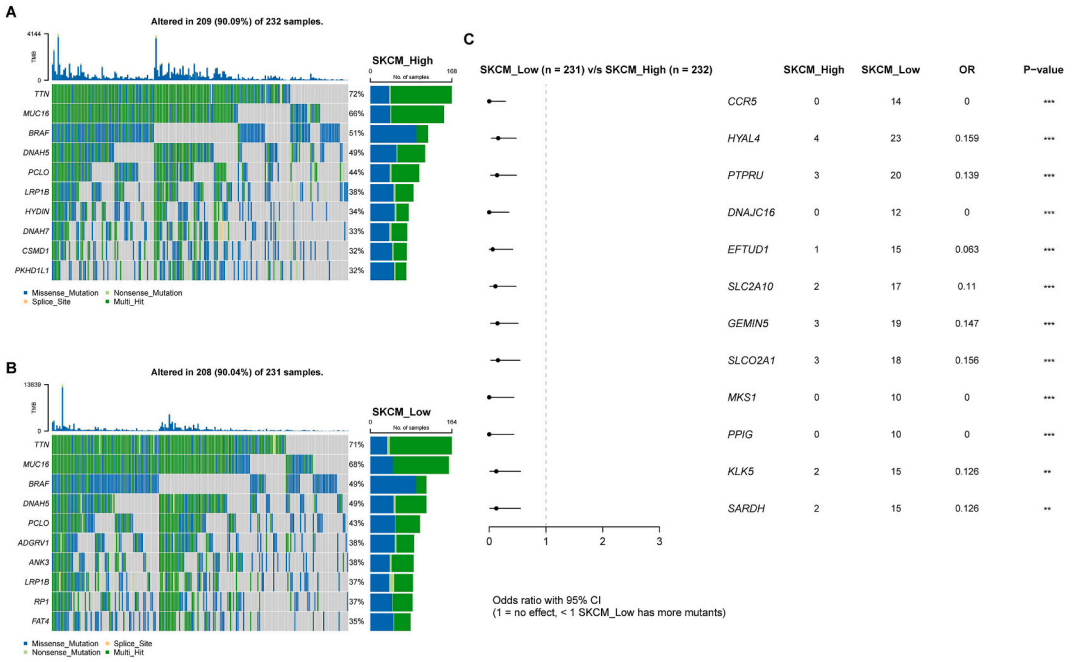

Fig. 8. Higher arginine biosynthesis score indicates lower genetic mutations in SKCM. Oncoplots for the mutation distribution of TOP 10 mutated genes in SKCM_High group (A) and SKCM_Low group (B). Blue represents Missense_Mutation; green represents Multi_Hit; light green represents Nonsense_Mutation; yellow represents Splice_Site. (C) Forest plot for comparison of gene mutation frequency in SKCM_High and SKCM_Low groups. OR indicates odds ratio; OR<1 means the mutation frequency is higher in the SKCM-Low group; ** indicates $p \leq 0.01$, *** indicates $p \leq 0.001$. (For interpretation of the references to color in this figure legend, the reader is referred to the Web version of this article.)

insensitive to immunotherapy. In addition, we obtained SKCM data and divided the samples into high- and low-score groups, and we found that the incidence of gene mutations was high (>90%) in both groups of samples; the top five genes with the highest mutation frequency were the same in both groups: TTN, MUC16, BRAF, DNAH5, and PCLO (Fig. 8A and B). Comparisons between the two groups showed that the mutation frequency in the SKCM_low group was significantly higher than that in the SKCM_high group (Fig. 8C), suggesting that targeted therapy may be an effective treatment modality for patients with SKCM.

3.6. Bulk and single-cell RNA-seq data indicated that the arginine biosynthesis score is associated with immunotherapy outcomes

Samples containing transcriptome data and the data for therapeutic responses to immunotherapies, including PD-1 and PD-L1 blockade, were obtained as external datasets (GSE61676, GSE135222, and NCT02684006) to validate the utility of arginine biosynthesis scores in predicting survival outcomes and immunotherapeutic response. Higher arginine biosynthesis scores were associated with poorer prognosis and lower immunotherapy response rates in advanced lung cancer (Fig. 9A and B) and renal clear cell carcinoma (Fig. 9C). Four single-cell RNA-seq datasets (GSE115978, GSE120575, GSE123813, and GSE145281) were used to assess the expression profiles of arginine biosynthesis genes in multiple cell types. As illustrated in Fig. 10, different cell types were identified in SKCM (Fig. 10A and B), BCC (Fig. 10C), and BLCA (Fig. 10D), respectively, with T cells, B cells, and NK cells as the dominant immune cell types; arginine biosynthesis genes were generally expressed at lower levels in these cells and at higher levels in endothelial cells and monocyte macrophages, and a further evaluation of arginine biosynthesis scores showed the same trend. To verify the relationship between arginine biosynthesis scores and immunotherapy response, we divided the samples in each dataset into two groups on the basis of immunotherapy efficacy and compared the differences in arginine biosynthesis scores between the two groups; the scores were significantly higher in patients who did not respond to immunotherapy (Fig. 11A–D), consistent with the results obtained from the bulk RNA-seq datasets. In the four single-cell RNA-seq datasets, with the UMAP dimensionality reduction, the cells were divided into 5–10 different cell types; the response to immune checkpoint blockade therapy was divided into two subclusters (no response/response), which were visualized with different color degrees; and arginine biosynthesis scores were categorized as high or low (Fig. 12A–C, E, G). The arginine biosynthesis scores of all cell types were relatively low. The bar plots showed a lower percentage of B and T cells in the high-scoring group (Fig. 12B–D, F, H). We then employed GSVA enrichment analysis to score the hallmark pathways. In all cells, arginine biosynthesis scores were positively related to these pathways, including the metabolic and immune-related glycolysis, adipogenesis, and complement pathways. A detailed description of specific cell types yielded different results, with arginine biosynthesis scores in B and T cells being mostly negatively correlated with pathways, indicating that different cells function differently (Fig. 13A–D).

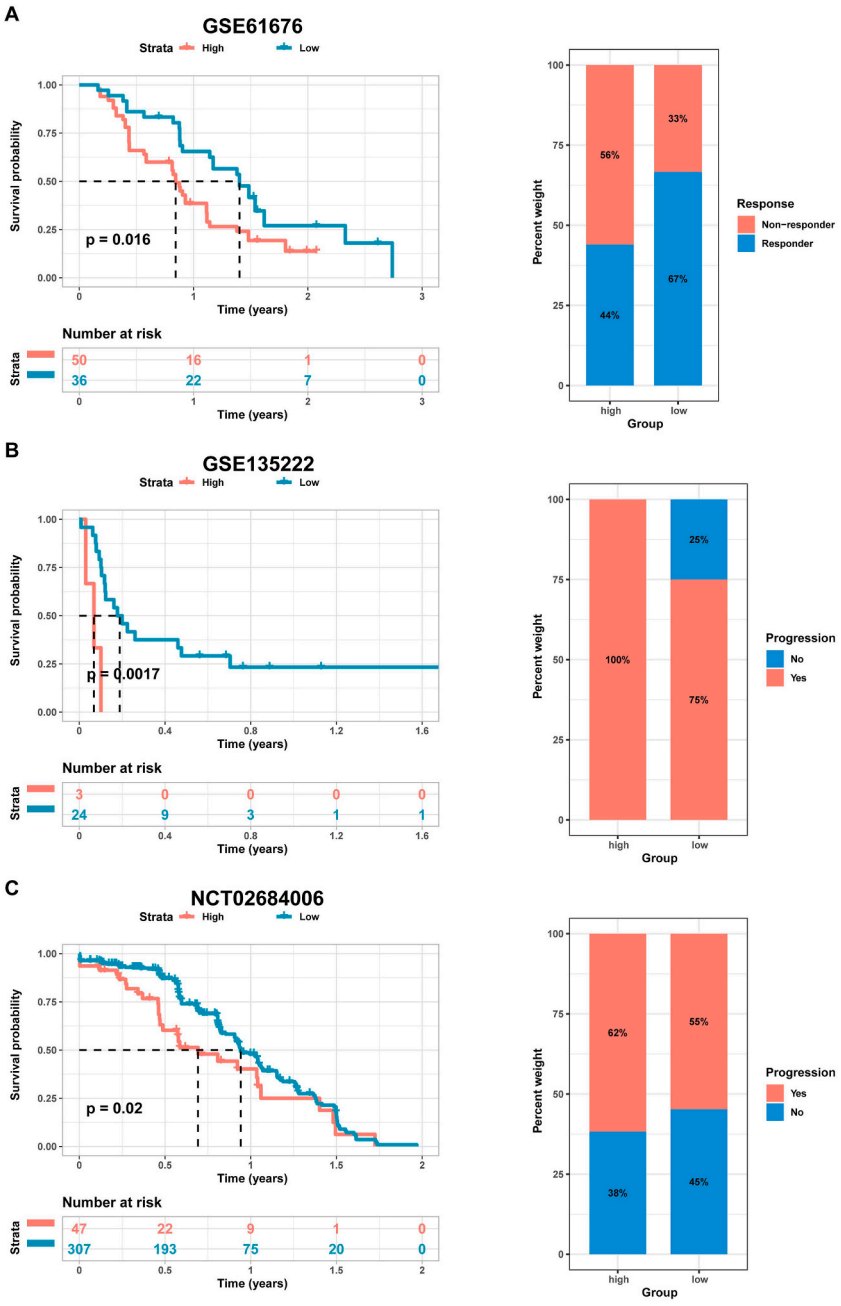

Fig. 9. Patients with higher arginine biosynthesis scores present a poorer prognosis for immunotherapy. Kaplan–Meier plots (left) for the survival differences and bar plots (right) for response rate or progression rate between high and low arginine biosynthesis score group for immunotherapy in the GSE61676 dataset (n = 86) (A), GSE135222 dataset (n = 27) (B), and NCT02684006 dataset (n = 354) (C). Red represents the high arginine biosynthesis score group, and light blue represents the low arginine biosynthesis score group in Kaplan–Meier plots. Red represents non-responder and disease progression, blue represents responder and no disease progression in bar plots. (For interpretation of the references to color in this figure legend, the reader is referred to the Web version of this article.)

3.7. Prediction of potential therapeutic targets among arginine biosynthesis genes using the GSCA database

Because high-scoring patients are not sensitive to immunotherapy, the sensitivity to immunotherapy may be increased by targeting the relevant pathways. Therefore, to identify potential therapeutic targets and compounds for patients with high arginine biosynthesis scores, we screened two drug response databases (CTRP and GDSC) and found that low expression of GOT1, GOT2, GLUL, GLUD1, GLUD2, GLS2, ASS1, and ARG1, and high expression of GLS were associated with resistance to targeted therapy for erlotinib (Fig. 14A).

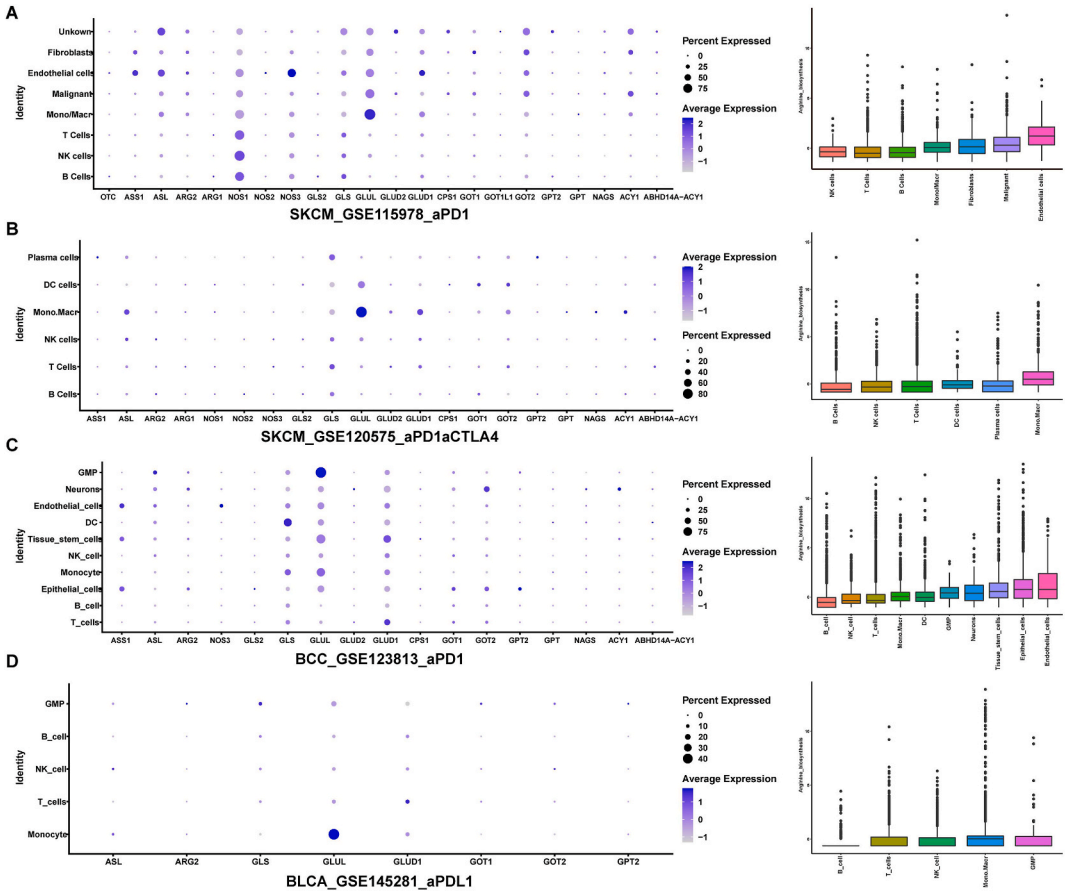

Fig. 10. Arginine biosynthesis genes are generally lowly expressed in T, B, and NK cells in various cancers. Bubble plots (left) for the expression of arginine biosynthesis genes and bar plots (right) for arginine biosynthesis score of multiple cell types in the GSE115978 dataset (A), GSE120575 dataset (B), GSE123813 dataset (C), and GSE145281 dataset (D). The size of the dot indicates the percentage of gene expression; blue indicates the average expression level of the gene, and the darker the color the higher the expression level in bubble plots. (For interpretation of the references to color in this figure legend, the reader is referred to the Web version of this article.)

In addition, the correlation between arginine biosynthesis genes and the estimated IC50 values of compounds from GDSC was evaluated using Pearson correlation analysis. After filtering with an FDR less than 0.05, eight candidate compounds were identified. Specifically, we found that a low expression level of ARG1 is associated with resistance to targeted therapies (Fig. 14B).

3.8. Validation of genes using immunohistochemistry and in vitro assays

The real-time quantitative polymerase chain reaction results revealed statistically significant differences in gene expression between normal tissues and tumors (Supplementary Fig. 4A and B). Immunohistochemistry experiments were performed to validate these results at the translational level (Supplementary Fig. 4C and D). The mRNA and protein expression levels of these two genes were consistent.

4. Discussion

Arginine metabolism has been associated with a range of biological processes that contribute to cancer progression and has been linked to the prognosis and immune microenvironment of many tumors. However, the roles of the 22 arginine biosynthetic genes in cancers remain unclear. This study comprehensively analyzed large-scale bulk RNA-seq, scRNA-seq, and epigenomic data to investigate the role of arginine biosynthesis genes in 33 cancer types and to uncover crucial biological observations of hallmarks and pathways.

Endogenous arginine is taken up by cancer cells to facilitate cancer cell growth and metastasis; however, cancer cells cannot synthesize arginine from metabolic intermediates [21], rendering them endogenous arginine-deficient. Previous studies have identified the importance of arginine deprivation in cancer therapy not only for its direct cytotoxic effects on cancer cells, but also for its capacity to induce cell cycle arrest [22,23]. While arginine synthesis is associated with the gene expression of several enzymes, we

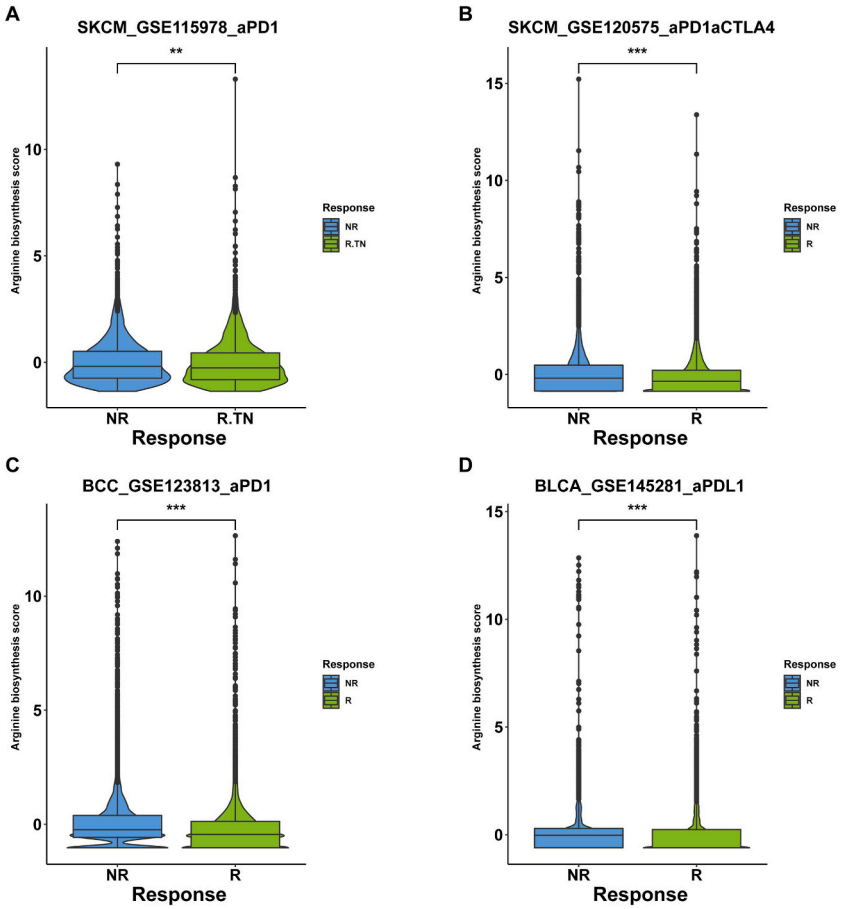

Fig. 11. Higher arginine biosynthesis score predicts a lower immunotherapy response rate. Violin plots for arginine biosynthesis scores of different immunotherapy responses in the GSE115978 dataset (A), GSE120575 dataset (B), GSE123813 dataset (C), and GSE145281 dataset (D). NR represents non-responder; R represents responder; blue indicates NR; green indicates R; ** indicates $p \leq 0.01$, *** indicates $p \leq 0.001$. (For interpretation of the references to color in this figure legend, the reader is referred to the Web version of this article.)

separately analyzed the differential expression of each of the 22 arginine biosynthesis genes in different types of cancer and found that while their expression and prognostic impact were not homogeneous, they widely correlated with each other.

We classified the arginine biosynthesis genes on the basis of the biological processes associated with the GO terms in the PPI network. Among these, ASL, OTC, ASS1, and NAGS are the key genes involved in arginine synthesis and are also associated with arginine metabolism, along with NOS1, NOS2, NOS3, ARG2, ARG1, ASL, and CPS1, which are also closely related to NO production and metabolism. Among the remaining genes, GPT, GLS, GLS2, GLUL, GLUD1, GLUD2, GOT1, and GOT2 are mainly involved in the synthesis and metabolism of glutamate, which can be used to synthesize arginine through the ornithine cycle, so the synthesis and metabolism of glutamate is associated with the synthesis of arginine as well. On the basis of the study by Li et al. [24], we calculated arginine biosynthesis scores to comprehensively evaluate the contribution of arginine biosynthesis genes in multiple cancers and found that arginine biosynthesis scores were risk factors for SKCM, THYM, and MESO, and patients with high-score SKCM had worse OS, DSS, and PFI. Wu et al. [21] reported that arginine deficiency enhances the sensitivity of melanoma to tumor necrosis factor-related apoptosis-inducing ligand therapy, suggesting that arginine metabolism is associated with tumor prognosis and drug resistance.

Based on these observations, we further investigated the potential underlying mechanisms. First, we analyzed individual genes at the transcriptomic and epigenomic levels. Genetic alterations significantly affect gene expression regulation and cancer progression [25,26]. The frequency of SNVs in arginine biosynthesis genes was as high as 81.93%, with the highest frequency of mutations in NOS1 at 26%; thus, targeting this gene may be beneficial in improving tumor prognosis, as demonstrated in a previous study that targeted NOS1 to inhibit ovarian cancer progression and reduce cisplatin resistance in OVCAR3 cell lines [27]. Furthermore, in terms of methylation modifications, the negative association between RNA expression levels and methylation status in the majority of genes indicates that promoter methylation is ubiquitous for these genes [28], and methylation inhibitors could be used as therapeutic agents, especially for ACY1.

Next, we performed GSVA to explore the relationship between the enriched pathways and the arginine biosynthesis score. We observed that the arginine biosynthesis score was negatively correlated with several immune-related pathways, such as the IL6 Jak/

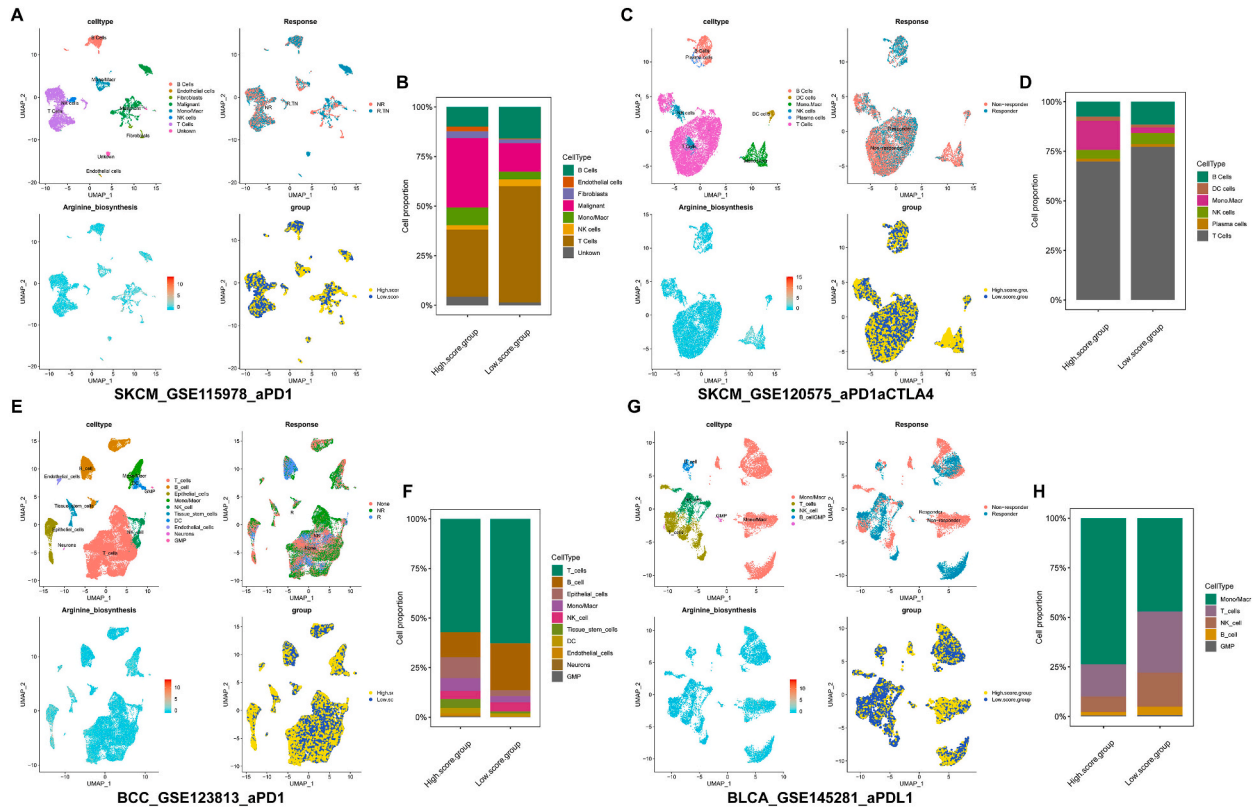

Fig. 12. The lower proportion of B and T cells in the high arginine biosynthesis score group. UMAP plots for the distribution and dissimilarity of the cell type, immunotherapy response, arginine biosynthesis score, and arginine biosynthesis score group in the GSE115978 dataset (n = 31) (A), GSE120575 dataset (n = 48) (C), GSE123813 dataset (n = 14) (E), and GSE145281 dataset (n = 10) (G). Bar plots for the proportion of cell type in the High_score and Low_score group in the GSE115978 dataset (n = 31) (B), GSE120575 dataset (n = 48) (D), GSE123813 dataset (n = 14) (F), and GSE145281 dataset (n = 10) (H).

Stat3 signaling pathway, NF-κB signaling pathway, Notch signaling pathway, Wnt β-catenin signaling pathway, and TGF-β signaling pathway. The IL-6/mIL-6Rα complex is involved in early immune responses through activation of JAK and phosphorylation of STAT3 [29], and in patients with breast cancer, activation of the IL6 Jak/Stat3 signaling pathway promotes cancer metastasis and suppresses antitumor immune responses [30]. The NF-κB signaling pathway is involved in biological functions in immune cell and lymphoid organ development, immune homeostasis, and immune response [31]. Similarly, the Notch signaling pathway plays a vital role in developing and maintaining immune responses and facilitating appropriate responses to pathogens [32]. Non-T-cell-inflamed tumors exhibit massive activation of the Wnt/β-catenin signaling pathway in ovarian cancer. The Wnt/β-catenin signaling pathway is negatively correlated with T-cell activity [33,34]. During tumor progression, the TGF-β signaling pathway acts as a suppressor of adaptive and innate immune responses and functions as an effective mechanism of immune evasion in a diverse range of cancers [35]. Patients with higher arginine biosynthesis scores showed greater suppression of antitumor immunity, which may be the predominant factor responsible for the worse prognosis of high-scoring patients. Accordingly, we analyzed the tumor microenvironment and immune cell infiltration. We noticed a significant negative correlation between the arginine biosynthesis score and Stromalcore and ImmuneScore in multiple cancers and a lower degree of immune cell infiltration in high-score patients, implying that high-score patients had an immune desert-type tumor microenvironment.

Therefore, we hypothesized that patients with high arginine biosynthesis scores would be insensitive to immunotherapy. We first performed a correlation analysis, and the results showed a negative correlation between the arginine biosynthesis score and immune checkpoint expression levels in several cancer types. As expected, patients with high arginine biosynthesis scores had significantly lower immunotherapy response rates and worse prognoses than those with low scores, and these findings were confirmed in several external bulk RNA-seq datasets. With the evolution of single-cell technology, an increasing number of studies have used it to exploit the heterogeneity of single cells [36]. In the present study, single-cell RNA-seq datasets were used to evaluate the molecular characteristics of tumor-infiltrating immune cells in the tumor microenvironment. The patients with high scores showed a significantly lower ratio of B and T cells than those with low scores, and the results of GSVA suggested that B and T cells were negatively correlated with multiple immune-related pathways, illustrating that immune evasion in high-score patients was mainly mediated by reduced activation of T and B cells, which is consistent with the findings reported by Kim et al. [37]. Similarly, we verified, as evidenced by scRNA-seq, that the rate of resistance to immunotherapy was significantly higher in the high-score group than in the low-score group, consistent with the

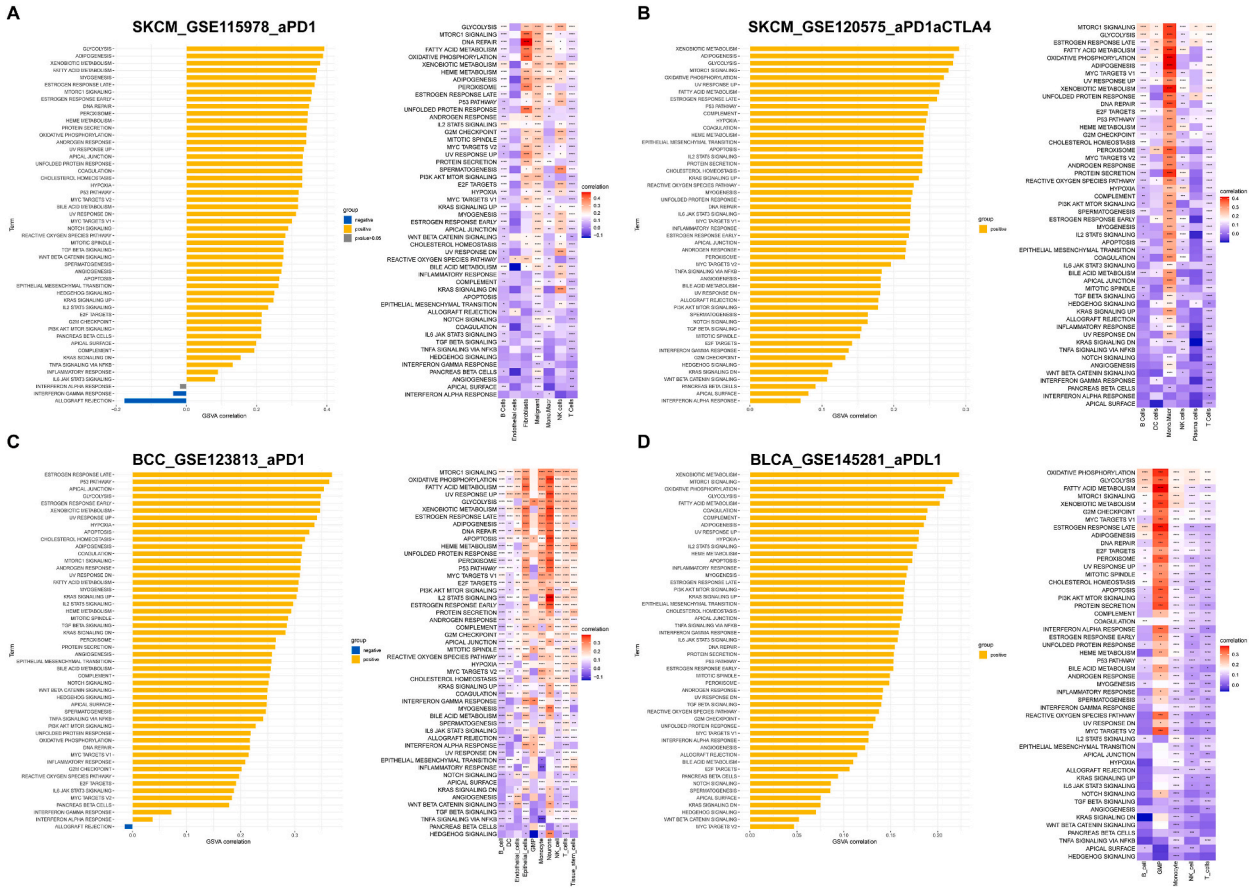

Fig. 13. The correlation between arginine biosynthesis score and enriched pathways in single-cell RNA-seq datasets. Bar plots (left) for the correlation between arginine biosynthesis score and hallmark pathways in all cell types and heatmaps (right) for the correlation between arginine biosynthesis score and hallmark pathways in different cell types in GSE115978 dataset (A), GSE120575 dataset (B), GSE123813 dataset (C), and GSE145281 dataset (D). Blue indicates a positive correlation; yellow indicates a negative correlation; grey indicates $p > 0.05$ in bar plots. Red indicates a positive correlation; blue indicates a negative correlation; the darker the color, the stronger the correlation in heatmaps. * indicates $p \leq 0.05$, ** indicates $p \leq 0.01$, *** indicates $p \leq 0.001$, and **** indicates $p \leq 0.0001$. (For interpretation of the references to color in this figure legend, the reader is referred to the Web version of this article.)

results of bulk RNA-seq, indicating that immune checkpoint blockade therapy is more appropriate for low-score patients.

Immunotherapy was less effective in patients with high arginine biosynthesis scores. Inspired by the study by Wu et al. [21], which enhanced immunotherapy sensitivity using targeted drugs, we immediately predicted the targeted drugs for the arginine metabolic pathway. These results indicate that elevated expression levels of ASS1 are associated with resistance to multiple drugs, and that targeting ASS1 may be an effective therapeutic option for patients with high arginine biosynthesis scores. ASS1, a key rate-limiting enzyme for arginine metabolism, can promote arginine deprivation by targeting ASS1 in SCLC, and arginine-depleting agents combined with PD-1/PD- L1 immune checkpoint inhibitors can further improve the survival of patients with SCLC [38]. Taken together, we demonstrated that arginine biosynthesis genes are associated with tumor immune evasion and therapy resistance across different types of cancer and that the combination of arginine-depleting agents and immunotherapy may improve the drug resistance status of patients with tumors.

Despite these promising findings, this study had several limitations. The seven RNA-seq datasets of the immune checkpoint blockade cohorts included in our studies covered only five cancer types (NSCLC, KIRC, SKCM, BCC, and BLCA), and some clinical annotation data were not available in some of the RNA-seq datasets. Moreover, the findings regarding the role of arginine biosynthesis genes in immunotherapy in this study were based on bioinformatics analysis. Further real-world studies are required to verify the potential mechanisms underlying arginine biosynthesis and immune evasion.

5. Conclusions

In summary, we systematically described the role of arginine biosynthesis genes in the tumor immune microenvironment, revealed their relationship with immunotherapy resistance, and showed that a combination of immunotherapy and drugs targeting arginine

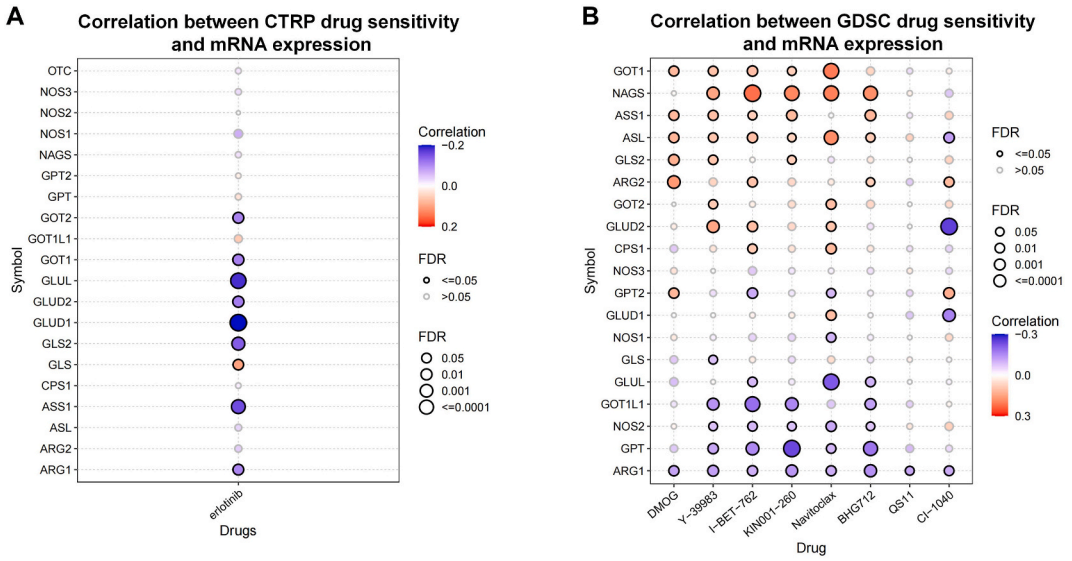

Fig. 14. The correlation between mRNA expression of arginine biosynthesis genes and CTRP/GDSC drug sensitivity. Bubble plot for the correlation between gene expression and the sensitivity of CTRP drug (A) and GDSC drug (B) in pan-cancer. FDR represents false discovery rate; the size of the dot indicates the value of FDR, the larger the FDR value the larger the dot; red indicates positive correlation; blue indicates negative correlation; the darker the color, the stronger the correlation. (For interpretation of the references to color in this figure legend, the reader is referred to the Web version of this article.)

biosynthesis-related genes may improve the prognosis of patients with high arginine biosynthesis scores. Further investigation is needed in future research.

Data availability statement

The analyzed datasets generated during the study are available from the corresponding author upon reasonable request.

Funding sources

This work was supported by the National Natural Science Foundation of China (No. 82060464) and the Yunnan Provincial Department of Science and Technology (Kun Medical Joint Special) Science and Technology Plan Project (202001AY070001-061 and 202201AY070001-108).

CRediT authorship contribution statement

Zhiyong Tan: Data curation. **Haihao Li:** Methodology. **Yinglong Huang:** Investigation. **Shi Fu:** Data curation. **Haifeng Wang:** Writing – review & editing. **Jiansong Wang:** Writing – review & editing.

Declaration of competing interest

The authors declare that they have no known competing financial interests or personal relationships that could have appeared to influence the work reported in this paper.

Acknowledgments

We thank the Gene Expression Omnibus (GEO) and The Cancer Genome Atlas (TCGA) databases for sharing large amounts of their data. We thank Prof. Mingxia Ding for his involvement in formulating the study design and concepts.

Appendix A. Supplementary data

Supplementary data to this article can be found online at https://doi.org/10.1016/j.heliyon.2024.e26804.

References

[1] B. Wang, X. Rong, E.N.D. Palladino, J. Wang, A.M. Fogelman, M.G. Martín, W.A. Alrefai, D.A. Ford, P. Tontonoz, Phospholipid Remodeling and Cholesterol Availability regulate Intestinal Stemness and tumorigenesis, Cell Stem Cell 22 (2018) 206–220.e4, https://doi.org/10.1016/j.stem.2017.12.017.

[2] R. Keshet, A. Erez, Arginine and the metabolic regulation of nitric oxide synthesis in cancer, Dis Model Mech 11 (2018) dmm033332, https://doi.org/10.1242/dmm.033332.

[3] G. Capuano, N. Rigamonti, M. Grioni, M. Freschi, M. Bellone, Modulators of arginine metabolism support cancer immunosurveillance, BMC Immunol. 10 (2009) 1, https://doi.org/10.1186/1471-2172-10-1.

[4] S. Ostrand-Rosenberg, Immune surveillance: a balance between protumor and antitumor immunity, Curr. Opin. Genet. Dev. 18 (2008) 11–18, https://doi.org/10.1016/j.gde.2007.12.007.

[5] M. Nowak, M. Klink, The role of tumor-associated macrophages in the progression and chemoresistance of ovarian cancer, Cells 9 (2020) 1299, https://doi.org/10.3390/cells9051299.

[6] A. Matos, M. Carvalho, M. Bicho, R. Ribeiro, Arginine and arginases modulate metabolism, tumor microenvironment and prostate cancer progression, Nutrients 13 (2021) 4503, https://doi.org/10.3390/nu13124503.

[7] P.C. Rodriguez, D.G. Quiceno, J. Zabaleta, B. Ortiz, A.H. Zea, M.B. Piazuelo, A. Delgado, P. Correa, J. Brayer, E.M. Sotomayor, S. Antonia, J.B. Ochoa, A. C. Ochoa, Arginase I production in the tumor microenvironment by mature myeloid cells inhibits T-cell receptor expression and antigen-specific T-cell responses, Cancer Res. 64 (2004) 5839–5849, https://doi.org/10.1158/0008-5472.CAN-04-0465.

[8] N. Avtandilyan, H. Javrushyan, G. Petrosyan, A. Trchounian, The involvement of arginase and nitric oxide synthase in breast cancer development: arginase and NO synthase as therapeutic targets in cancer, 2018, BioMed Res. Int. (2018) 8696923, https://doi.org/10.1155/2018/8696923.

[9] I. Bednarz-Misa, M.G. Fleszar, P. Fortuna, Ł. Lewandowski, M. Mierzchała-Pasierb, D. Diakowska, M. Krzystek-Korpacka, Altered L-arginine metabolic pathways in gastric cancer: potential therapeutic targets and Biomarkers, Biomolecules 11 (2021) 1086, https://doi.org/10.3390/biom11081086.

[10] C.-L. Chen, S.-C. Hsu, T.-Y. Chung, C.-Y. Chu, H.-J. Wang, P.-W. Hsiao, S.-D. Yeh, D.K. Ann, Y. Yen, H.-J. Kung, Arginine is an epigenetic regulator targeting TEAD4 to modulate OXPHOS in prostate cancer cells, Nat. Commun. 12 (2021) 2398, https://doi.org/10.1038/s41467-021-22652-9.

[11] D. Massi, C. Marconi, A. Franchi, F. Bianchini, M. Paglierani, S. Ketabchi, C. Miracco, M. Santucci, L. Calorini, Arginine metabolism in tumor-associated macrophages in cutaneous malignant melanoma: evidence from human and experimental tumors, Hum. Pathol. 38 (2007) 1516–1525, https://doi.org/10.1016/j.humpath.2007.02.018.

[12] M.J. Goldman, B. Craft, M. Hastie, K. Repečka, F. McDade, A. Kamath, A. Banerjee, Y. Luo, D. Rogers, A.N. Brooks, J. Zhu, D. Haussler, Visualizing and interpreting cancer genomics data via the Xena platform, Nat. Biotechnol. 38 (2020) 675–678, https://doi.org/10.1038/s41587-020-0546-8.

[13] D. Szklarczyk, A.L. Gable, D. Lyon, A. Junge, S. Wyder, J. Huerta-Cepas, M. Simonovic, N.T. Doncheva, J.H. Morris, P. Bork, L.J. Jensen, C. von Mering, STRING v11: protein-protein association networks with increased coverage, supporting functional discovery in genome-wide experimental datasets, Nucleic Acids Res. 47 (2019) D607–D613, https://doi.org/10.1093/nar/gky1131.

[14] S. Hänzelmann, R. Castelo, J. Guinney, GSVA: gene set variation analysis for microarray and RNA-seq data, BMC Bioinf. 14 (2013) 7, https://doi.org/10.1186/1471-2105-14-7.

[15] D. Zeng, M. Li, R. Zhou, J. Zhang, H. Sun, M. Shi, J. Bin, Y. Liao, J. Rao, W. Liao, Tumor microenvironment Characterization in gastric cancer Identifies prognostic and Immunotherapeutically relevant gene Signatures, Cancer Immunol. Res. 7 (2019) 737–750, https://doi.org/10.1158/2326-6066.CIR-18-0436.

[16] D. Sun, J. Wang, Y. Han, X. Dong, J. Ge, R. Zheng, X. Shi, B. Wang, Z. Li, P. Ren, L. Sun, Y. Yan, P. Zhang, F. Zhang, T. Li, C. Wang, TISCH: a comprehensive web resource enabling interactive single-cell transcriptome visualization of tumor microenvironment, Nucleic Acids Res. 49 (2021) D1420–D1430, https://doi.org/10.1093/nar/gkaa1020.

[17] R.J. Motzer, P.B. Robbins, T. Powles, L. Albiges, J.B. Haanen, J. Larkin, X.J. Mu, K.A. Ching, M. Uemura, S.K. Pal, B. Alekseev, G. Gravis, M.T. Campbell, K. Penkov, J.L. Lee, S. Hariharan, X. Wang, W. Zhang, J. Wang, A. Chudnovsky, A. di Pietro, A.C. Donahue, T.K. Choueiri, Avelumab plus axitinib versus sunitinib in advanced renal cell carcinoma: biomarker analysis of the phase 3 JAVELIN Renal 101 trial, Nat Med 26 (2020) 1733–1741, https://doi.org/10.1038/s41591-020-1044-8.

[18] S.I. Khater, M.F. Dowidar, A.E. Abdel-Aziz, T. Khamis, N. Dahran, L.S. Alqahtani, M.M.M. Metwally, A.S. Al-Hady Abd-Elrahamn, M. Alsieni, M.E. Alosaimi, M. H. Abduljabbar, A.A. Mohamed. β -Cell Autophagy Pathway and Endoplasmic Reticulum Stress Regulating-Role of Liposomal Curcumin in Experimental Diabetes Mellitus: A Molecular and Morphometric Study, Antioxidants (Basel). 11 (2022) 2400. https://doi.org/10.3390/antiox11122400.

[19] N. Dahran, Y.M. Abd-Elhakim, A.A. Mohamed, M.M. Abd-Elsalam, E.N. Said, M.M.M. Metwally, A.E. Abdelhamid, B.A. Hassan, M. Alsieni, M.E. Alosaimi, M. H. Abduljabbar, Palliative effect of Moringa olifera-mediated zinc oxide nanoparticles against acrylamide-induced neurotoxicity in rats, Food Chem Toxicol 171 (2023) 113537, https://doi.org/10.1016/j.fct.2022.113537.

[20] K. Yoshihara, M. Shahmoradgoli, E. Martínez, R. Vegesna, H. Kim, W. Torres-Garcia, V. Treviño, H. Shen, P.W. Laird, D.A. Levine, S.L. Carter, G. Getz, K. Stemke-Hale, G.B. Mills, R.G.W. Verhaak, Inferring tumour purity and stromal and immune cell admixture from expression data, Nat Commun 4 (2013) 2612. https://doi.org/10.1038/ncomms3612.

[21] C. Wu, M. You, D. Nguyen, M. Wangpaichitr, Y.-Y. Li, L.G. Feun, M.T. Kuo, N. Savaraj, Enhancing the Effect of Tumor Necrosis Factor-Related Apoptosis-Inducing Ligand Signaling and Arginine Deprivation in Melanoma, Int J Mol Sci 22 (2021) 7628. https://doi.org/10.3390/ijms22147628.

[22] H. Al-Koussa, N. El Mais, H. Maalouf, R. Abi-Habib, M. El-Sibai, Arginine deprivation: a potential therapeutic for cancer cell metastasis? A review, Cancer Cell Int 20 (2020) 150. https://doi.org/10.1186/s12935-020-01232-9.

[23] G. Nasreddine, M. El-Sibai, R.J. Abi-Habib, Cytotoxicity of [HuArgI (co)-PEG5000]-induced arginine deprivation to ovarian Cancer cells is autophagy dependent, Invest New Drugs. 38 (2020) 10- 19. https://doi.org/10.1007/s10637-019-00756-w.

[24] J. Li, Z. Wu, S. Wang, C. Li, X. Zhuang, Y. He, J. Xu, M. Su, Y. Wang, W. Ma, D. Fan, T. Yue, A necroptosis-related prognostic model for predicting prognosis, immune landscape, and drug sensitivity in hepatocellular carcinoma based on single-cell sequencing analysis and weighted co-expression network, Front Genet 13 (2022) 984297. https://doi.org/10.3389/fgene.2022.984297.

[25] E. Heitzer, P. Ulz, J.B. Geigl, M.R. Speicher, Non-invasive detection of genome-wide somatic copy number alterations by liquid biopsies, Mol Oncol 10 (2016) 494–502. https://doi.org/10.1016/j.molonc.2015.12.004.

[26] Y. Pan, G. Liu, F. Zhou, B. Su, Y. Li, DNA methylation profiles in cancer diagnosis and therapeutics, Clin Exp Med 18 (2018) 1–14. https://doi.org/10.1007/s10238-017-0467-0.

[27] Z. Zou, X. Li, Y. Sun, L. Li, Q. Zhang, L. Zhu, Z. Zhong, M. Wang, Q. Wang, Z. Liu, Y. Wang, Y. Ping, K. Yao, B. Hao, Q. Liu, NOS1 expression promotes proliferation and invasion and enhances chemoresistance in ovarian cancer, Oncol Lett 19 (2020) 2989–2995. https://doi.org/10.3892/ol.2020.11355.

[28] Q. Zhang, R. Huang, H. Hu, L. Yu, Q. Tang, Y. Tao, Z. Liu, J. Li, G. Wang, Integrative Analysis of Hypoxia-Associated Signature in Pan-Cancer, iScience 23 (2020) 101460. https://doi.org/10.1016/j.isci.2020.101460.

[29] D.C. Chonov, M.M.K. Ignatova, J.R. Ananiev, M.V. Gulubova, IL-6 Activities in the Tumour Microenvironment. Part 1, Open Access Maced J Med Sci 7 (2019) 2391–2398. https://doi.org/10.3889/oamjms.2019.589.

[30] S.G. Manore, D.L. Doheny, G.L. Wong, H.-W. Lo, IL-6/JAK/STAT3 Signaling in Breast Cancer Metastasis: Biology and Treatment, Front Oncol 12 (2022) 866014. https://doi.org/10.3389/fonc.2022.866014.

[31] H. Yu, L. Lin, Z. Zhang, H. Zhang, H. Hu, Targeting NF-κB pathway for the therapy of diseases: mechanism and clinical study, Signal Transduct Target, Ther 5 (2020) 209. https://doi.org/10.1038/s41392-020-00312-6.

[32] R.C. Castro, R.A. Gonçales, F.A. Zambuzi, F.G. Frantz, Notch signaling pathway in infectious diseases: role in the regulation of immune response, Inflamm Res 70 (2021) 261–274. https://doi.org/10.1007/s00011-021-01442-5.

[33] J.A. Wall, S. Meza-Perez, C.B. Scalise, A. Katre, A.I. Londoño, W.J. Turbitt, T. Randall, L.A. Norian, R.C. Arend, Manipulating the Wnt/β-catenin signaling pathway to promote anti-tumor immune infiltration into the TME to sensitize ovarian cancer to ICB therapy, Gynecol Oncol 160 (2021) 285–294. https://doi.org/10.1016/j.ygyno.2020.10.031.

[34] J.J. Luke, R. Bao, R.F. Sweis, S. Spranger, T.F. Gajewski, WNT/β-catenin Pathway Activation Correlates with Immune Exclusion across Human Cancers, Clin Cancer Res. 25 (2019) 3074–3083. https://doi.org/10.1158/1078-0432.CCR- 18- 1942.
[35] E. Batlle, J. Massagué, Transforming Growth Factor-β Signaling in Immunity and Cancer, Immunity 50 (2019) 924–940. https://doi.org/10.1016/j.immuni.2019.03.024.
[36] B. Hwang, J.H. Lee, D. Bang, Single-cell RNA sequencing technologies and bioinformatics pipelines, Exp Mol Med 50 (2018) 1–14. https://doi.org/10.1038/s12276-018-0071-8.
[37] S.-H. Kim, J. Roszik, E.A. Grimm, S. Ekmekcioglu, Impact of l-arginine metabolism on immune response and Anticancer immunotherapy, Front. Oncol. 8 (2018) 67. https://doi.org/10.3389/fonc.2018.00067.
[38] J. Carpentier, I. Pavlyk, U. Mukherjee, P.E. Hall, P.W. Szlosarek, Arginine deprivation in SCLC: mechanisms and Perspectives for therapy, Lung Cancer 13 (2022) 53–66. https://doi.org/10.2147/LCTT.S335117.